

Journal Pre-proofs

Design and synthesis of novel 1-substituted 3-(6-phenoxy pyridin-3-yl)-1*H*-pyrazolo[3,4-*d*]pyrimidin-4-amine analogs as selective BTK inhibitors for the treatment of mantle cell lymphoma

Fansheng Ran, Yang Liu, Shengping Yu, Kaiwen Guo, Wendi Tang, Xin Chen, Guisen Zhao

PII: S0045-2068(19)30631-5
DOI: <https://doi.org/10.1016/j.bioorg.2019.103367>
Reference: YBIOO 103367

To appear in: *Bioorganic Chemistry*

Received Date: 23 April 2019
Revised Date: 16 September 2019
Accepted Date: 14 October 2019

Please cite this article as: F. Ran, Y. Liu, S. Yu, K. Guo, W. Tang, X. Chen, G. Zhao, Design and synthesis of novel 1-substituted 3-(6-phenoxy pyridin-3-yl)-1*H*-pyrazolo[3,4-*d*]pyrimidin-4-amine analogs as selective BTK inhibitors for the treatment of mantle cell lymphoma, *Bioorganic Chemistry* (2019), doi: <https://doi.org/10.1016/j.bioorg.2019.103367>

This is a PDF file of an article that has undergone enhancements after acceptance, such as the addition of a cover page and metadata, and formatting for readability, but it is not yet the definitive version of record. This version will undergo additional copyediting, typesetting and review before it is published in its final form, but we are providing this version to give early visibility of the article. Please note that, during the production process, errors may be discovered which could affect the content, and all legal disclaimers that apply to the journal pertain.

© 2019 Published by Elsevier Inc.



Design and synthesis of novel 1-substituted 3-(6-phenoxy pyridin-3-yl)-1*H*-pyrazolo[3,4-*d*]pyrimidin-4-amine analogs as selective BTK inhibitors for the treatment of mantle cell lymphoma

Fansheng Ran^{a†}, Yang Liu^{b†}, Shengping Yu^a, Kaiwen Guo^a, Wendi Tang^a, Xin Chen^a, Guisen Zhao^{a,*}

^a Department of Medicinal Chemistry, Key Laboratory of Chemical Biology (Ministry of Education), School of Pharmaceutical Sciences, Shandong University, Jinan, Shandong 250012, PR China

^b Department of Lymphoma and Myeloma, The University of Texas MD Anderson Cancer Center, Houston, TX 77030, USA

[†]These authors contributed equally to this work.

* Corresponding author: Guisen Zhao

E-mail: guisenzhao@sdu.edu.cn

Abstract

Ibrutinib (**IBN**), a first-in-class BTK-inhibitor, was approved by the FDA for the treatment of mantle cell lymphoma (MCL). Although **IBN** shows excellent performance as an anti-lymphoma agent, it has some undesirable side effects due to its off-target activities. Our studies yielded a novel series of 3-(6-phenoxy pyridin-3-yl)-4-amine-1*H*-pyrazolo[3,4-*d*]pyrimidine derivatives capable of potent inhibition of Bruton's tyrosine kinase (BTK). Notably, compound **13e** explained potent BTK inhibitory activity and could completely inhibit the phosphorylation of BTK and PLC γ 2 in Z138 cells at low micromolar concentration. Compared with **IBN**, compound **13e** improved anti-proliferative activities 3-40 folds in MCL cell lines with IC₅₀ values lower than 1 μ M. Low micromolar doses of **13e** could induce strong cell apoptosis in Jeko-1 and Z138 cells. In addition, compound **13e** showed greater BTK selectivity and higher stability in human liver microsomes than **IBN** and potential safety improvement for the treatment of MCL.

Keywords:

Mantle cell lymphoma; BTK; Docking; Anticancer; Selectivity

1. Introduction

Bruton's tyrosine kinase (BTK), a member of the Tec kinase family, is expressed in many hematopoietic cells, including myeloid cells and B cells, but not in T cells¹⁻³. BTK plays a critical role in B-cell receptor (BCR) signaling pathway, which regulates cell survival, proliferation, activation, differentiation and maturation of B cells⁴⁻⁷. The deregulation of BTK has been observed in numerous B-cell-derived malignancies, including mantle cell lymphoma (MCL), chronic lymphocytic leukemia (CLL) and acute lymphoblastic leukemia (ALL)^{6, 8-9}.

MCL, a subtype of Non-Hodgkin's Lymphoma (NHL) with poor prognosis, is responsible for 7% of NHL¹⁰. BTK is commonly overexpressed in MCL, and the BCR signaling pathway is implicated in the pathogenesis of MCL¹¹⁻¹². In 2013, the first-in-class BTK-inhibitor ibrutinib (**IBN**, **1**) was approved by FDA for the treatment of MCL¹³⁻¹⁵. Although **IBN** shows excellent performance as an anti-lymphoma agent, it has some undesirable side effects due to its unexpected off-target toxicities resulting from potential binding to non-target locations¹⁶. In addition to targeting BTK, **IBN** interacts with several kinases involved in other important signaling pathways, such as EGFR, ErbB2, ErbB4, Itk, Lyn, Yes, Hck, and PTK5¹⁷⁻¹⁹.

We performed molecular docking using Sybyl X 2.0 to investigate the interactions between **IBN** and BTK (PDB code: 5P9I). As shown in **Fig 1A**, the pyrazolopyrimidine core occupied the ATP binding pocket, performing several important interactions with the hinge region. The primary amine directly formed hydrogen bond with the backbone carbonyl of Glu475, and the N-3 nitrogen of the pyrimidine ring formed a hydrogen bond interaction with the amine of Met477. The carbonyl group formed a hydrogen bond with the amine of Cys481. The diphenyl ether group extended to the hydrophobic pocket behind the gatekeeper Thr474 and the distal phenyl group displayed an edge-to-face aromatic interaction with the phenyl of Phe540. Moreover, there were many hydrogen bond donors around the ring A of **IBN**, such as the amino group of Lys430 with 2.70 Å distance and the hydroxy group of Ser538 with 2.96 Å distance. If we introduce a hydrogen bond acceptor at the A ring, potential hydrogen bond interactions may be formed with Ser538 or/and Lys430 with the

improvement of the selectivity on BTK²⁰. Therefore, we introduced a nitrogen atom as a hydrogen bond acceptor at the 3'-position of ring A and optimized the substituents at the N-1 position of pyrazolopyrimidine to obtain a novel series of 3-(6-phenoxyphenyl)-4-amine-1*H*-pyrazolo[3,4-*d*]pyrimidine BTK inhibitors.

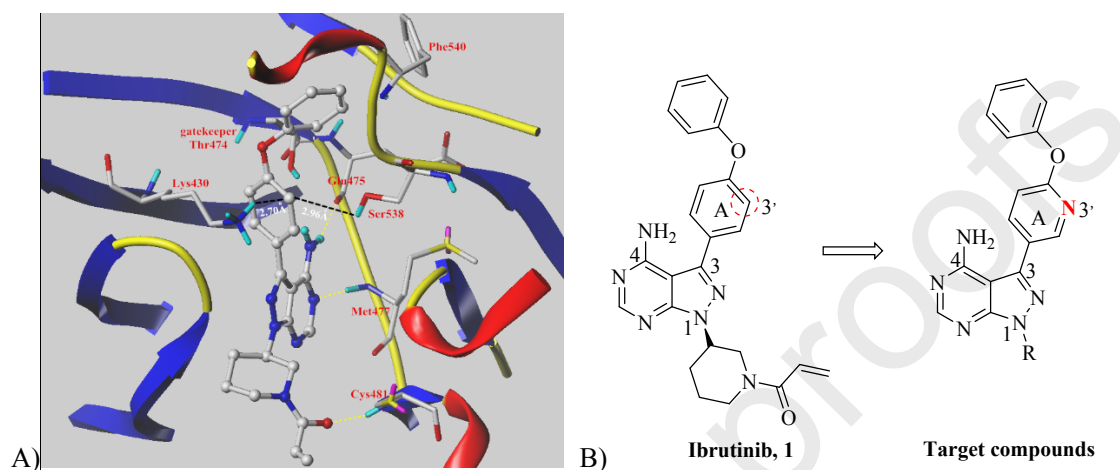
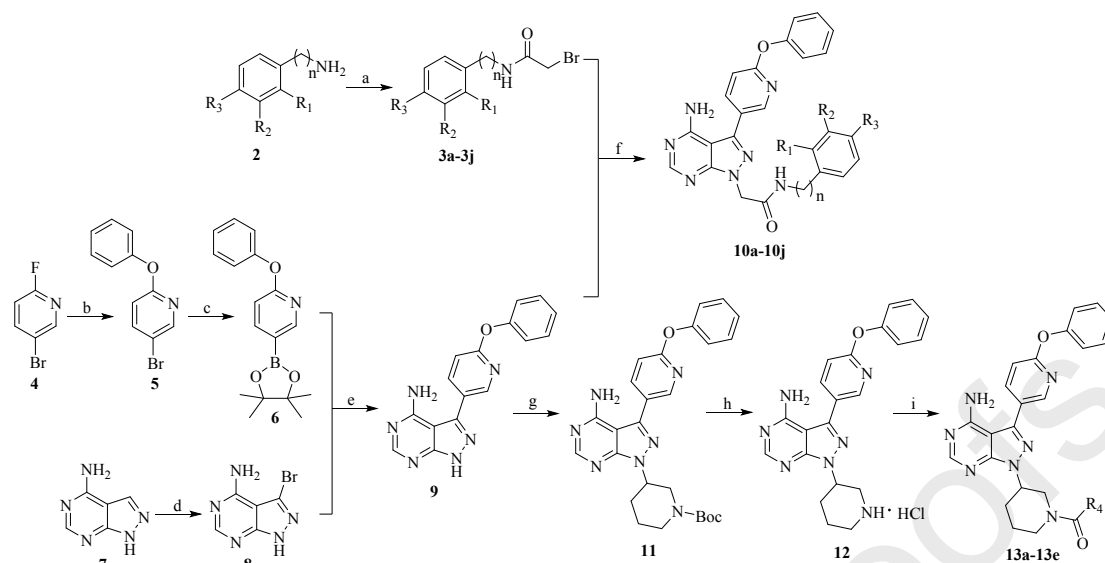


Figure 1. (A) Molecular docking mode of IBN with BTK. PDB ID:5P9I. (B) Design of the target compounds.

2. Results and discussion

2.1. Chemistry

The synthetic routes for these compounds are explained in **Scheme 1**. Condensation of various substituted amines (**2**) with bromoacetyl bromide afforded compounds **3a-3j**. Nucleophilic aromatic substitution of compound **4** with phenol under the presence of sodium hydride provided the compound **5**. Subsequent coupling of compound **5** with bis(pinacolato)diboron catalyzed by palladium acetate afforded compound **6**. Bromination of compound **7** by *N*-bromosuccinimide (NBS) provided the compound **8**, which reacted with compound **6** through Suzuki reaction to provide compound **9**. *N*-alkylation of compound **9** with compounds **3a-3j** gave the target compounds **10a-10j**. Compound **9** was transformed to racemic compounds **11** with racemic 1-Boc-3-hydroxypiperidine by the Mitsunobu reaction, which were deprotected in HCl/1,4-dioxane and subsequently reacted with different acyl chlorides or substituted acids to produce target compounds **13a-13e**.

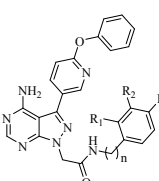
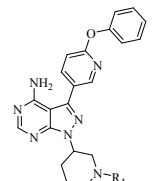


Scheme 1. Synthetic route of series **10** and **13**. Reagents and conditions: (a) NaHCO₃, bromoacetyl bromide, ethyl acetate:H₂O = 1:1, r.t., 1h; (b) Phenol, NaH, THF, 80°C, 12h; (c) Pd(OAc)₂, X-PHOS, KOAc, bis(pinacolato)diboron, 1,4-dioxane, 90°C, 12h; (d) NBS, DMF, 90°C, 1h; (e) Pd(PPh₃)₄, K₃PO₄, 1,4-dioxane:H₂O = 4:1, 120°C, 24h; (f) K₂CO₃, DMF, r.t., 5h; (g) 1-Boc-3-hydroxypiperidine (racemate), PPh₃, DIAD, 0°C to r.t., 5h; (h) HCl\1,4-dioxane, r.t., 5h; (i) Acyl chlorides, Et₃N, THF, 0°C to r.t., 5h or substituted acids, HBTU, Et₃N, r.t., 8h.

2.2. BTK inhibition activity

The newly synthesized pyrazolopyrimidine analogs were evaluated for their activity against BTK via a KinaseProfiler radiometric protein kinase assay. As shown in **Table 1**, series **10** remained BTK residual activity more than 70% at 1μM. It was found that the inhibitory activities of series **10** were not increased with either extending the chain length (**10a**, **10b** and **10c**) or changing the groups on the terminal benzene ring (**10d-10j**). It implied that introduction of a substituted acetamide at the N-1 position of the pyrazolopyrimidine core might not be a preferred approach. For series **13**, when the group at R₄ position was a hydroxyacetyl group, 2-hydroxypropionyl group, hydroxy tert-butanoyl group or methoxypropionyl group respectively, these compounds (**13a-13d**) showed weak inhibitory activities against BTK. Notably, compound **13e** with a chloroacetyl group at R₄ position increased significantly the BTK inhibitory activity that is consistent with the finding reported²¹.

Table 1. The effects of series **10** and **13** on BTK activity.

Structure	Code	n	R ₁	R ₂	R ₃	R ₄	BTK residue	BTK IC ₅₀ (nM)
							activity (%) at 1 μM	
	IBN	-	-	-	-	-	-1	8
	10a	0	H	F		-	92	ND ^a
	10b	1	H	F	H	-	89	ND ^a
	10c	2	H	H	F	-	101	ND ^a
	10d	0	F	F	F	-	79	ND ^a
	10e	0	H	Cl	F	-	98	ND ^a
	10f	0	H	Cl	CN	-	80	ND ^a
	10g	0	F	Cl	H	-	91	ND ^a
	10h	0	H	CF ₃	Br	-	101	ND ^a
	10i	0	H	CF ₃	CN	-	97	ND ^a
	10j	0	H	H	Me	-	87	ND ^a
	13a	-	-	-	-		80	ND ^a
	13b	-	-	-	-		77	ND ^a
	13c	-	-	-	-		72	ND ^a
	13d	-	-	-	-		83	ND ^a
	13e	-	-	-	-		5	36

ND^a: not detected.

2.3. Cell viability activity

According to the CellTiter-Glo Luminescent cell viability assay, compound **13e** was determined for their anti-proliferative activity in MCL cell lines and primary MCL patient cells. The tested MCL cell lines included Mino, Jeko-1, Z138, and Maver-1. As shown in **Table 2**, compound **13e** showed potent effect against MCL cells with IC₅₀ values lower than 1 μM, which is 3-39 folds higher than **IBN**. As shown in **Fig 2A**, **13e** also demonstrated more potent antiproliferative activity in primary MCL patient cells than **IBN**. Compound **13e** exhibited robust antiproliferative effects in both MCL cell lines and primary patient tumor cells.

Table 2. Cell proliferation assay assessing the effects of compounds on MCL cell lines.

Code	Cell viability assay, IC ₅₀ μM			
	Mino	Jeko-1	Z138	Maver-1
IBN	15.7	1.1	9.7	7.80
13e	0.4	0.4	0.4	0.4

2.4. Inhibitory effects on BTK signaling

To further examine the inhibitory effects of **13e** on BTK signaling, immunoblotting was

performed to detect the phosphorylation of BTK and its downstream effector PLC γ 2 in Z138 cells. The results showed that **13e** treatment for 16 h completely inhibited the phosphorylation of BTK and PLC γ 2 at 0.5 μ M (**Fig 2B**). These results suggested that **13e** behaved strong inhibitory effect on BTK signaling pathway.

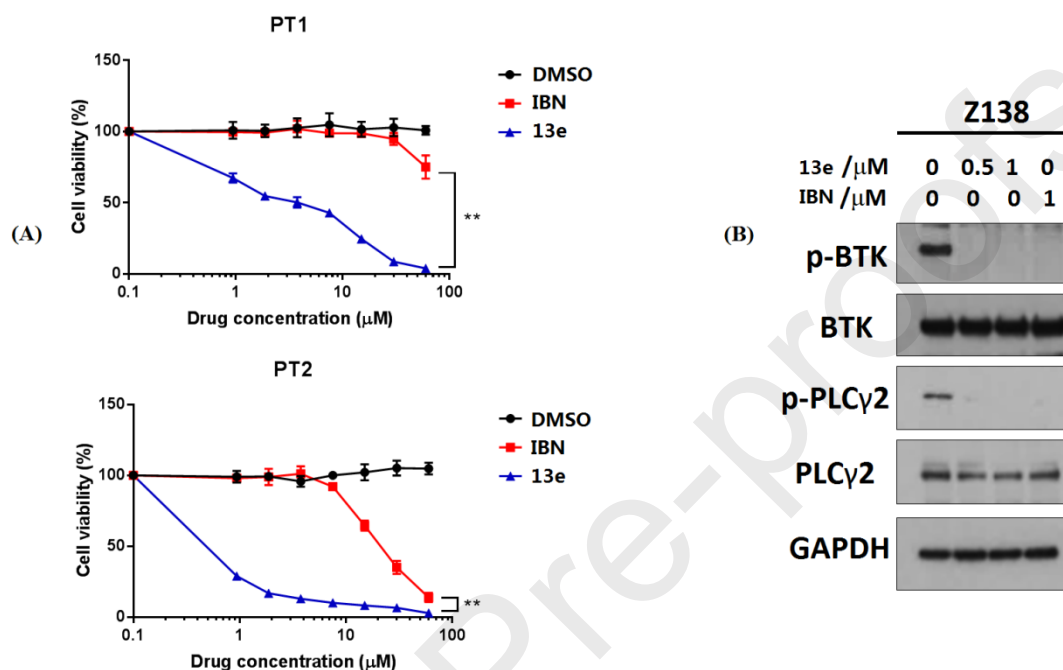


Figure 2. (A) Cell viability assay after 24 h treatment of **13e** and **IBN** in two naïve MCL patient cells. Statistical significance is indicated as **P < 0.01. (B) Effects of **13e** on BTK signaling in Z138 cells after 16 h treatment.

2.5. Cell apoptosis assay

We proceeded to test the effects of **13e** on apoptosis in Jeko-1 and Z138 cells via an annexin V-FITC/propidium iodide (PI) binding assay. As illustrated in **Fig 3**, after 24 h of treatment, **13e** triggered dose-dependent apoptosis of the cells with ratios of 35% and 69% at concentrations of 1 μ M and 2 μ M compared with 14% in non-treated Jeko-1 cells, and 19% and 82% at concentrations of 1 μ M and 2 μ M compared with 17% in non-treated Z138 cells.

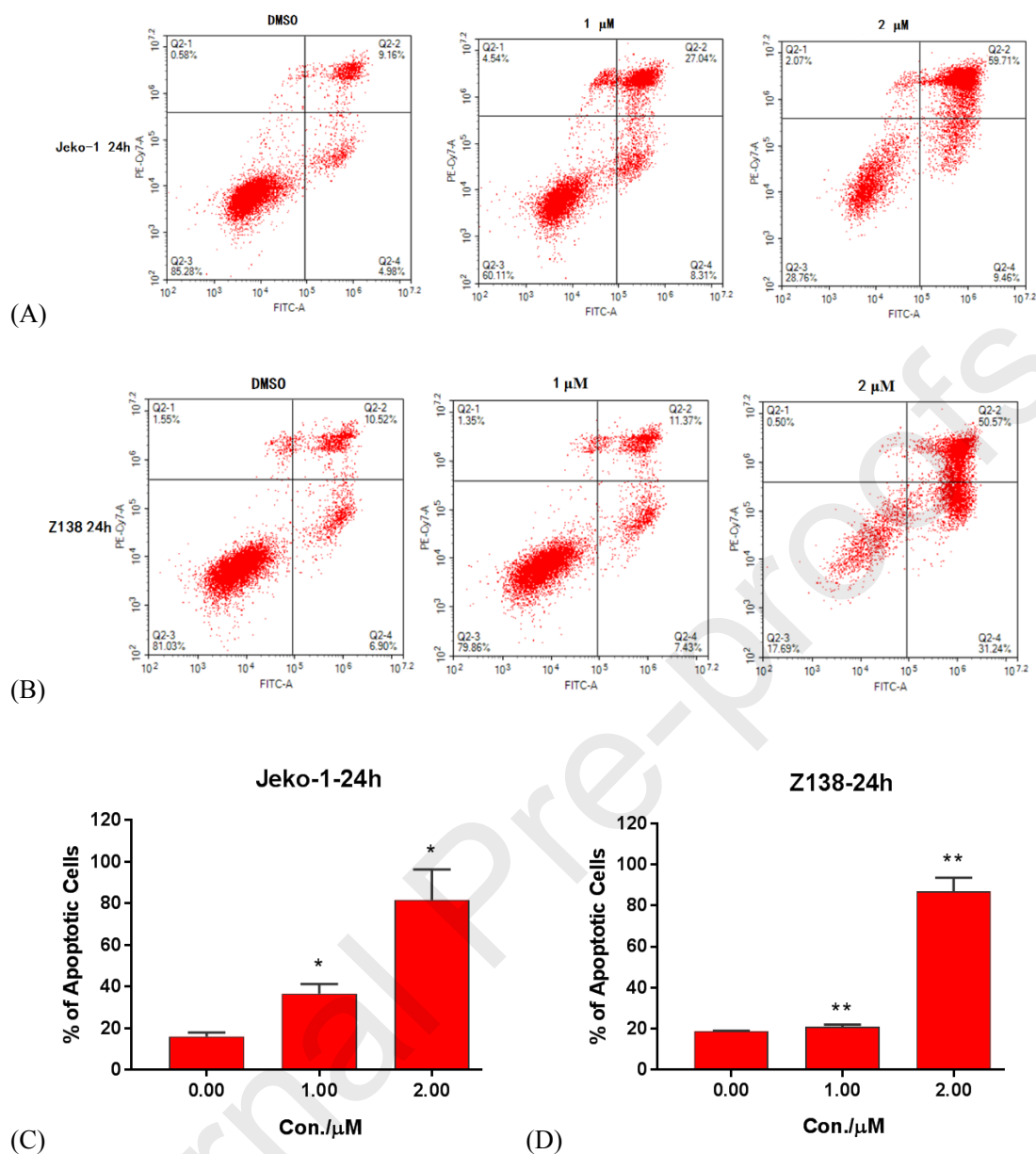


Figure 3. Cell apoptosis assay for **13e** in Jeko-1 and Z138 cells. **(A/C)** Apoptosis assay of **13e** at indicated concentrations in Jeko-1 cells for 24 h; **(B/D)** Apoptosis assay of **13e** at indicated concentrations in Z138 cells for 24 h. The data shown are the mean of three independent experiments. Statistical significance is indicated as * $P < 0.05$, ** $P < 0.01$ compared with the DMSO control.

2.6. Selectivity over other kinases

We further tested the biochemical activity of compound **13e** against a panel of 22 kinases. The major off-target kinases of **13e** were those with cysteine residue in the ATP binding pocket, which could be irreversibly bound by the covalent reactive group. As shown in **Table 3**, **13e** showed high potency against Blk, Bmx, Tec, Txk, ErbB4 and EGFR with IC_{50} values of 10, 6, 36, 104, 147 and

292 nM, respectively. Compared to **IBN**, **13e** showed much lower inhibitory effect against Brk, B-raf, Csk, Fgr, Flt3, Fyn, Itk, Hck, Lck, Lyn, PTK5, Src, SRM and Yes, indicating improved BTK selectivity and potential safety improvement for the treatment of MCL.

Table 3. Inhibition efficacy (%) among different kinases at 1 μ M by **13e** and **IBN**.

Kinases	13e	IBN	Kinases	13e	IBN
Blk	100% (10nM)	100%	Hck	16%	96%
Bmx	97% (6nM)	102%	Itk	12%	86%
Brk	33%	92%	JAK3	41%	54%
B-raf	-4%	19%	Lck	35%	99%
Csk	7%	87%	Lyn	-10%	99%
EGFR	77% (292nM)	98%	PTK5	-8%	91%
ErbB2	69% (948nM)	73%	Src	5%	96%
ErbB4	91% (147nM)	101%	SRM	19%	100%
Fgr	16%	92%	Tec	91% (36nM)	103%
Flt3	-27%	8%	Txk	83% (104nM)	97%
Fyn	16%	97%	Yes	-28%	102%

2.7. Stability in human liver microsomes

Compound **13e** was further evaluated its stability in human liver microsomes (**Table 4**). Higher metabolic stability was detected after a 60-min incubation, as evidenced by total remaining percentage (6.7%) for **13e**, while only 0.2% for **IBN** was left. Half-life ($T_{1/2}$) and intrinsic clearance ($CL_{int(mic)}$) values were calculated. **13e** showed longer half-life (16.8 min) and lower clearance (82.5 μ L/min/mg) compared with **IBN** ($T_{1/2}$ = 1.6 min, $CL_{int(mic)}$ = 846.7 μ L/min/mg).

Table 4. Metabolic stability of **IBN** and **13e** in human liver microsomes. R^2 is the correlation coefficient of the linear regression for the determination of kinetic constant, $T_{1/2}$ is half-life and $CL_{int(mic)}$ is the intrinsic clearance.

Sample Name	HLM 0.5					
	R^2	$T_{1/2}$ (min)	$CL_{int(mic)}$ (μ L/min/mg)	$CL_{int(liver)}$ (mL/min/kg)	Remaining (T=60 min)	Remaining (*NCF=60 min)
IBN	0.9975	1.6	846.7	762.0	0.2%	87.4%
13e	0.9070	16.8	82.5	74.2	6.7%	62.8%

2.8. Molecular modeling

The molecular modeling results of compound **13e** with BTK are shown in **Fig 4**. The pyrazolopyrimidine core formed several important hydrogen bonds with hinge region through

Glu475, Met477 and Cys481. The 6-phenoxy pyridine group extended to the hydrophobic pocket behind the gatekeeper Thr474 displaying an edge-to-face aromatic interaction with Phe540. As expected, N-1 nitrogen at pyridine ring formed a hydrogen bond with the amino of Lys430. This interaction could play an important role in kinase selectivity for **13e**.

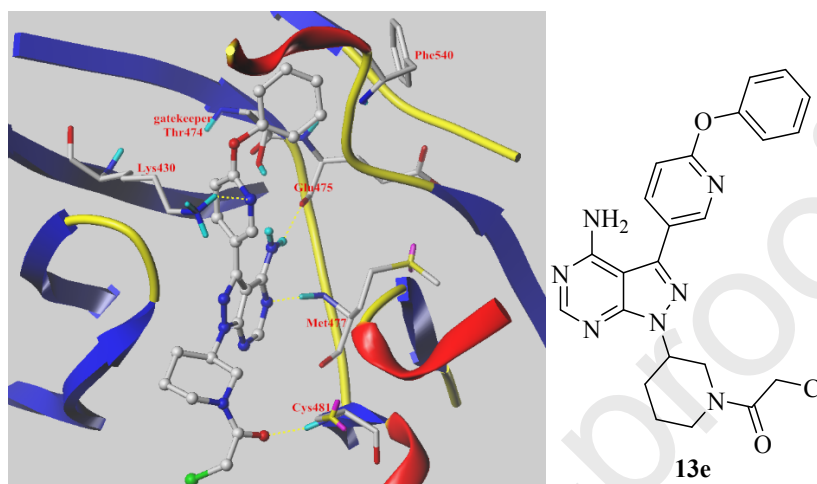


Figure 4. Docking pose of **13e** with BTK. PDB ID:5P9I.

3. Conclusion

In summary, this study outlined the design, synthesis, and biological evaluation of novel 3-(6-phenoxy pyridin-3-yl)-4-amino-1*H*-pyrazolo[3,4-*d*]pyrimidine derivatives as potential agents for treating MCL. Among these compounds, **13e** exhibited potent BTK inhibitory activity and could completely inhibit the phosphorylation of BTK and PLC γ 2 in Z138 cells at 0.5 μ M. Compared to **IBN**, **13e** exhibited robust antiproliferative effects in both mantle cell lymphoma cell lines and primary patient tumor cells. **13e** explained a dose-dependent apoptosis in Jeko-1 and Z138 cells. In addition, compound **13e** showed greater BTK selectivity and higher stability in human liver microsomes than **IBN** and potential safety improvement for the treatment of MCL, indicating **13e** would be a promising candidate in cancer therapy.

4. Experimental section

4.1. Chemistry

All the chemical reagents and solvents were purchased from commercial sources and used without further purification. Reactions were monitored using thin-layer chromatography (TLC)

performed on SGF254 plates. Column chromatography was carried out with the indicated solvents using silica gel (60 Å, 200 - 300 mesh). Melting points were determined using Büchi capillary melting point apparatus (Büchi Labortechnik AG, Switzerland) without correction. Using tetramethylsilane (TMS) as an internal standard in DMSO-*d*₆ or CDCl₃, NMR spectra were recorded at 400 MHz for ¹H and 100 MHz for ¹³C on a Bruker Avance DRX-400 Spectrometer (Bruker, Germany). The chemical shifts (δ) were reported in parts per million (ppm) using tetramethylsilane as internal standard.

4.2. General synthesis of compounds

4.2.1. General procedure for the synthesis of **3a-3j**

To a stirred solution of various substituted amines **2** (10 mmol) and NaHCO₃ (3.10 g, 37 mmol) in the mixed solution of ethyl acetate/water = 1/1 (20 mL), bromoacetyl bromide (3.84 g, 23 mmol) was added at room temperature. The mixture was stirred at room temperature for 1 h. After completion of the reaction, the reaction mixture was extracted with ethyl acetate. The organic layer was dried over Na₂SO₄ and the solvent was evaporated in vacuo to give **3a-3j**.

4.2.2. 5-Bromo-2-phenoxy pyridine (**5**)

To a solution of phenol (2.82 g, 30 mmol) in anhydrous tetrahydrofuran (THF) (20 mL) was slowly added 60% sodium hydride (0.96 g, 40 mmol). The mixture was stirred for 30 min at room temperature. 5-Bromo-2-fluoropyridine (**4**) (3.52 g, 20 mmol) was added and the reaction was heated to 80 °C for 12 h. After cooling down to room temperature, the mixture was poured into water and extracted with ethyl acetate. The organic phase was washed with brine, dried on Na₂SO₄, filtered, evaporated and the crude product was purified by silica gel column chromatography (petroleum ether/ethyl acetate, 100/1) yielding intermediate **5** as a colorless oil (4.4 g, 88%). ¹H NMR (400 MHz, DMSO-*d*₆) δ 8.27 (d, *J* = 2.4 Hz, 1H), 8.06 (dd, *J* = 8.7, 2.6 Hz, 1H), 7.47 - 7.39 (m, 2H), 7.23 (t, *J* = 7.4 Hz, 1H), 7.18 - 7.12 (m, 2H), 7.04 (d, *J* = 8.7 Hz, 1H).

4.2.3. 2-Phenoxy-5-(4,4,5,5-tetramethyl-1,3,2-dioxaborolan-2-yl)pyridine (**6**)

A premixed and degassed solution of Pd(OAc)₂ (154.60 mg, 0.69 mmol) and X-Phos (656.00 mg, 1.38 mmol) in dioxane (5 mL) that had been stirred for 20 minutes, was added to a stirred,

degassed mixture of bis(pinacolato)diboron (6.99 g, 27.50 mmol), potassium acetate (4.05 g, 41.30 mmol) and compound **5** (3.44 g, 13.77 mmol) in dioxane (50 mL). The mixture was stirred at 90 °C for 12 h. Upon completion, the reaction mixture was filtered and concentrated in vacuo. The residue was purified by silica gel column chromatography (petroleum ether/ethyl acetate, 30/1) to afford intermediate **6** as a white solid (3.06 g, 75%). ¹H NMR (400 MHz, DMSO-*d*₆) δ 8.36 (d, *J* = 1.5 Hz, 1H), 8.03 (dd, *J* = 8.3, 2.0 Hz, 1H), 7.43 (t, *J* = 7.9 Hz, 2H), 7.24 (t, *J* = 7.4 Hz, 1H), 7.14 (d, *J* = 7.7 Hz, 2H), 7.00 (d, *J* = 8.3 Hz, 1H), 1.30 (s, 12H).

4.2.4. 3-Bromo-1*H*-pyrazolo[3,4-*d*]pyrimidin-4-amine (**8**)

N-bromosuccinimide (6.65 g, 37.35 mmol) was added to a stirred solution of 1*H*-pyrazolo[3,4-*d*]pyrimidin-4-amine (**7**) (5.04 g, 37.35 mmol) in *N,N*-dimethylformamide (DMF) (30 mL). The reaction was heated at 90 °C for 1 h. Upon completion, the reaction was quenched with water (400 mL). The suspension was filtered and the filter cake was washed completely with water to yield compound **8** as a yellow solid (6.71 g, 84%). ¹H NMR (400 MHz, DMSO-*d*₆) δ 13.77 (s, 1H), 8.18 (s, 1H).

4.2.5. 3-(6-Phenoxy-pyridin-3-yl)-1*H*-pyrazolo[3,4-*d*]pyrimidin-4-amine (**9**)

The Pd(PPh₃)₄ (0.48 g, 0.41 mmol) was added to a mixture of compound **6** (2.97 g, 10 mmol), compound **8** (1.78 g, 8.33 mmol) and K₃PO₄ (3.53 g, 16.66 mmol) in the mixed solution of dioxane/water = 4/1 (50 mL). The mixture was degassed and put under nitrogen atmosphere, then was stirred at 120 °C for 24 h. After cooled to room temperature, the mixture was partitioned between ethyl acetate and water. The organic layer was separated and the aqueous layer was extracted. The combined organic phases were washed with brine, then dried and concentrated. The crude product was purified by silica gel column chromatography (dichloromethane/methanol, 80/1) to afford compound **9** as a white solid (1.92 g, 76%). ¹H NMR (400 MHz, DMSO-*d*₆) δ 13.67 (s, 1H), 8.38 (s, 1H), 8.23 (s, 1H), 8.08 (dd, *J* = 8.4, 1.8 Hz, 1H), 7.46 (t, *J* = 7.8 Hz, 2H), 7.27 - 7.15 (m, 4H), 6.94 (s, 2H).

4.2.6. General procedure for the synthesis of **10a-10j**

To a mixture of compound **9** (1 mmol) and K₂CO₃ (3.1 g, 1.5 mmol) in DMF (5 mL) was added compounds **3a-3j** (1.2 mmol) and the reaction mixture was stirred for 5 h at room temperature. The

reaction solution was poured into water (50 mL). The suspension was filtered and the crude product was purified by silica gel column chromatography (dichloromethane/methanol, 150/1-60/1) to yield target compounds **10a-10j**.

4.2.6.1. *4-(2-(4-Amino-3-(6-phenoxy pyridin-3-yl)-1H-pyrazolo[3,4-d]pyrimidin-1-yl)acetamido)-2-fluoro-N-methylbenzamide (10a)* White solid, yield 74%, Mp:208-210 °C, ¹H NMR (400 MHz, DMSO-*d*₆) δ 10.86 (s, 1H), 8.41 (d, *J* = 7.9 Hz, 1H), 8.28 (d, *J* = 10.6 Hz, 1H), 8.11 (s, 2H), 7.72 - 7.59 (m, 2H), 7.52 - 7.42 (m, 2H), 7.35 (t, *J* = 8.3 Hz, 1H), 7.31 - 6.92 (m, 6H), 5.29 (s, 2H), 2.77 (s, 3H). ¹³C NMR (100 MHz, DMSO-*d*₆) δ 166.31, 163.90, 163.49, 161.10, 158.74, 158.65, 156.54, 155.72, 154.32, 147.18, 142.45, 142.34, 141.58, 140.38, 131.45, 130.23, 125.11, 124.66, 121.60, 118.77, 118.63, 115.12, 112.27, 106.68, 106.39, 98.01, 50.25, 26.77. MS(ESI) *m/z*: 513.04 [M + H]⁺

4.2.6.2. *2-(4-Amino-3-(6-phenoxy pyridin-3-yl)-1H-pyrazolo[3,4-d]pyrimidin-1-yl)-N-(3-fluorobenzyl)acetamide (10b)* White solid, yield 80%, Mp:233-235 °C, ¹H NMR (400 MHz, DMSO-*d*₆) δ 8.75 (t, *J* = 5.9 Hz, 1H), 8.39 (d, *J* = 2.2 Hz, 1H), 8.27 (s, 1H), 8.08 (dd, *J* = 8.5, 2.4 Hz, 1H), 7.46 (t, *J* = 7.9 Hz, 2H), 7.37 (q, *J* = 7.5 Hz, 1H), 7.30 - 6.93 (m, 9H), 5.10 (s, 2H), 4.34 (d, *J* = 5.9 Hz, 2H). ¹³C NMR (100 MHz, DMSO-*d*₆) δ 167.09, 163.93, 163.43, 161.52, 158.71, 156.40, 155.54, 154.34, 147.17, 142.59, 142.52, 141.46, 140.34, 130.70, 130.62, 130.22, 125.09, 124.74, 123.58, 123.55, 121.56, 114.34, 114.12, 113.91, 112.24, 98.09, 49.77, 42.16. MS(ESI) *m/z*: 470.20 [M + H]⁺

4.2.6.3. *2-(4-Amino-3-(6-phenoxy pyridin-3-yl)-1H-pyrazolo[3,4-d]pyrimidin-1-yl)-N-(4-fluorophenethyl)acetamide (10c)* White solid, yield 82%, Mp:194-196 °C, ¹H NMR (400 MHz, DMSO-*d*₆) δ 8.38 (d, *J* = 2.1 Hz, 1H), 8.27 (s, 1H), 8.23 (t, *J* = 4.5 Hz, 1H), 8.07 (dd, *J* = 8.5, 2.3 Hz, 1H), 7.46 (t, *J* = 7.8 Hz, 2H), 7.37 - 6.97 (m, 10H), 4.97 (s, 2H), 3.30 (q, *J* = 6.8 Hz, 2H), 2.72 (t, *J* = 7.1 Hz, 2H). ¹³C NMR (100 MHz, DMSO-*d*₆) δ 166.69, 163.43, 162.51, 160.11, 158.68, 156.40, 155.53, 154.33, 147.17, 141.37, 140.35, 135.89, 135.86, 130.98, 130.90, 130.22, 125.09, 124.76, 121.57, 115.52, 115.31, 112.23, 98.01, 49.55, 40.87, 34.48. MS(ESI) *m/z*: 484.30 [M + H]⁺

4.2.6.4. *2-(4-Amino-3-(6-phenoxy pyridin-3-yl)-1H-pyrazolo[3,4-d]pyrimidin-1-yl)-N-(2,3,4-trifluorophenyl)acetamide (10d)* White solid, yield 78%, Mp:235-237 °C, ¹H NMR (400 MHz,

DMSO- d_6) δ 10.45 (s, 1H), 8.39 (d, $J = 1.9$ Hz, 1H), 8.27 (s, 1H), 8.09 (dd, $J = 8.5, 2.2$ Hz, 1H), 7.64 (q, $J = 6.2$ Hz, 1H), 7.46 (t, $J = 7.8$ Hz, 2H), 7.33 - 7.27 (m, 1H), 7.26 - 6.94 (m, 6H), 5.33 (s, 2H). ^{13}C NMR (100 MHz, DMSO- d_6) δ 166.38, 163.50, 158.74, 156.53, 155.72, 154.34, 148.74, 148.70, 148.62, 147.19, 146.28, 146.20, 146.18, 144.99, 144.88, 141.61, 140.98, 140.96, 140.37, 138.66, 138.52, 138.50, 138.36, 130.22, 125.10, 124.68, 124.06, 124.03, 123.97, 123.94, 121.58, 119.07, 119.05, 119.02, 118.98, 118.96, 112.47, 112.44, 112.26, 98.03, 49.84. MS(ESI) m/z : 492.04 $[\text{M} + \text{H}]^+$

4.2.6.5. *2-(4-Amino-3-(6-phenoxy pyridin-3-yl)-1H-pyrazolo[3,4-d]pyrimidin-1-yl)-N-(3-chloro-4-fluorophenyl)acetamide (10e)* White solid, yield 86%, Mp:213-215 °C, ^1H NMR (400 MHz, DMSO- d_6) δ 10.68 (s, 1H), 8.40 (d, $J = 2.3$ Hz, 1H), 8.27 (s, 1H), 8.09 (dd, $J = 8.5, 2.4$ Hz, 1H), 7.89 (dd, $J = 6.8, 2.4$ Hz, 1H), 7.48 - 7.38 (m, 4H), 7.26 - 6.99 (m, 6H), 5.26 (s, 2H). ^{13}C NMR (100 MHz, DMSO- d_6) δ 165.89, 163.47, 158.72, 156.51, 155.71, 154.94, 154.31, 152.53, 147.17, 141.55, 140.36, 136.26, 136.23, 130.22, 125.10, 124.66, 121.58, 121.11, 120.03, 119.97, 119.79, 119.61, 117.69, 117.47, 112.25, 98.00, 50.13. MS(ESI) m/z : 490.06 $[\text{M} + \text{H}]^+$

4.2.6.6. *2-(4-Amino-3-(6-phenoxy pyridin-3-yl)-1H-pyrazolo[3,4-d]pyrimidin-1-yl)-N-(3-chloro-4-cyanophenyl)acetamide (10f)* White solid, yield 74%, Mp:154-156 °C, ^1H NMR (400 MHz, DMSO- d_6) δ 11.10 (s, 1H), 8.40 (d, $J = 2.2$ Hz, 1H), 8.27 (s, 1H), 8.09 (dd, $J = 8.5, 2.4$ Hz, 1H), 8.02 (d, $J = 1.7$ Hz, 1H), 7.93 (d, $J = 8.6$ Hz, 1H), 7.61 (dd, $J = 8.6, 1.8$ Hz, 1H), 7.46 (t, $J = 7.9$ Hz, 2H), 7.35 - 6.94 (m, 6H), 5.32 (s, 2H). ^{13}C NMR (100 MHz, DMSO- d_6) δ 166.87, 163.49, 158.73, 156.56, 155.73, 154.30, 147.17, 144.23, 141.67, 140.36, 136.58, 135.83, 130.22, 125.11, 124.61, 121.59, 119.67, 118.35, 116.62, 112.26, 106.37, 97.99, 50.34. MS(ESI) m/z : 495.30 $[\text{M} - \text{H}]^-$

4.2.6.7. *2-(4-Amino-3-(6-phenoxy pyridin-3-yl)-1H-pyrazolo[3,4-d]pyrimidin-1-yl)-N-(3-chloro-2-fluorophenyl)acetamide (10g)* White solid, yield 81%, Mp:214-216 °C, ^1H NMR (400 MHz, DMSO- d_6) δ 10.42 (s, 1H), 8.40 (s, 1H), 8.28 (s, 1H), 8.10 (d, $J = 8.6$ Hz, 1H), 7.86 (t, $J = 7.5$ Hz, 1H), 7.46 (t, $J = 7.7$ Hz, 2H), 7.36 (t, $J = 8.4$ Hz, 1H), 7.33 - 7.13 (m, 6H), 7.12 - 6.90 (m, 1H), 5.35 (s, 2H). ^{13}C NMR (100 MHz, DMSO- d_6) δ 166.35, 163.47, 158.72, 156.53, 155.69, 154.30, 150.90, 148.43, 147.17, 141.57, 140.37, 130.22, 127.72, 127.62, 126.24, 125.54, 125.10, 124.66, 123.01, 121.59, 120.46, 120.30, 112.25, 97.99, 49.95. MS(ESI) m/z : 490.18 $[\text{M} + \text{H}]^+$

4.2.6.8. *2-(4-Amino-3-(6-phenoxy pyridin-3-yl)-1H-pyrazolo[3,4-d]pyrimidin-1-yl)-N-(4-bromo-3-(trifluoromethyl)phenyl)acetamide (10h)* White solid, yield 87%, Mp:118-120 °C, ¹H NMR (400 MHz, DMSO-*d*₆) δ 10.91 (s, 1H), 8.39 (d, *J* = 1.9 Hz, 1H), 8.27 (s, 1H), 8.18 (d, *J* = 2.0 Hz, 1H), 8.09 (dd, *J* = 8.5, 2.2 Hz, 1H), 7.84 (d, *J* = 8.7 Hz, 1H), 7.72 (d, *J* = 8.6 Hz, 1H), 7.46 (t, *J* = 7.8 Hz, 2H), 7.34 - 7.00 (m, 6H), 5.28 (s, 2H). ¹³C NMR (100 MHz, DMSO-*d*₆) 166.36, 163.49, 158.73, 156.53, 155.74, 154.32, 147.18, 141.62, 140.35, 138.91, 136.12, 130.21, 129.55, 129.25, 128.95, 128.64, 127.28, 125.09, 124.65, 124.56, 121.85, 121.57, 119.13, 118.66, 118.59, 112.42, 112.40, 112.26, 98.02, 50.24. MS(ESI) *m/z*: 584.00 [M + H]⁺

4.2.6.9. *2-(4-Amino-3-(6-phenoxy pyridin-3-yl)-1H-pyrazolo[3,4-d]pyrimidin-1-yl)-N-(4-cyano-3-(trifluoromethyl)phenyl)acetamide (10i)* White solid, yield 80%, Mp:132-134 °C, ¹H NMR (400 MHz, DMSO-*d*₆) δ 11.27 (s, 1H), 8.40 (d, *J* = 2.2 Hz, 1H), 8.27 (s, 2H), 8.13 (d, *J* = 8.6 Hz, 1H), 8.09 (dd, *J* = 8.5, 2.4 Hz, 1H), 7.95 (dd, *J* = 8.6, 1.6 Hz, 1H), 7.46 (t, *J* = 7.9 Hz, 2H), 7.36 - 6.97 (m, 6H), 5.34 (s, 2H). ¹³C NMR (100 MHz, DMSO-*d*₆) δ 167.09, 163.50, 158.73, 156.58, 155.74, 154.30, 147.17, 143.52, 141.71, 140.36, 137.14, 132.45, 132.13, 130.22, 125.11, 124.60, 124.19, 122.63, 121.59, 121.47, 117.09, 117.02, 116.97, 116.92, 116.97, 116.15, 112.26, 102.55, 98.00, 50.34. MS(ESI) *m/z*: 529.39 [M - H]⁻

4.2.6.10. *2-(4-Amino-3-(6-phenoxy pyridin-3-yl)-1H-pyrazolo[3,4-d]pyrimidin-1-yl)-N-(p-tolyl)acetamide (10j)* White solid, yield 79%, Mp:238-240 °C, ¹H NMR (400 MHz, DMSO-*d*₆) δ 10.33 (s, 1H), 8.39 (d, *J* = 1.8 Hz, 1H), 8.26 (s, 1H), 8.09 (dd, *J* = 8.5, 2.2 Hz, 1H), 7.45 (t, *J* = 7.1 Hz, 4H), 7.26 - 7.11 (m, 8H), 5.22 (s, 2H), 2.25 (s, 3H). ¹³C NMR (100 MHz, DMSO-*d*₆) δ 165.25, 163.46, 158.73, 156.47, 155.69, 154.35, 147.18, 141.41, 140.37, 136.57, 133.01, 130.23, 129.69, 125.09, 124.74, 121.58, 119.65, 112.26, 98.01, 50.16, 20.91. MS(ESI) *m/z*: 452.30 [M + H]⁺

4.2.7. *1-Boc-3-(4-amino-3-(6-phenoxy pyridin-3-yl)-1H-pyrazolo[3,4-d]pyrimidin-1-yl)piperidine (11)*

A mixture of compound **9** (1.83 g, 6.00 mmol), racemic 1-Boc-3-hydroxypiperidine (1.81 g, 6.00 mmol) and triphenylphosphine (PPh₃) (4.72 g, 18.00 mmol) in absolute anhydrous THF (25 mL) was stirred for 30 min under ice-cold conditions. Diisopropyl azodiformate (DIAD) (3.64 g, 18.00 mmol) was added dropwise to the reaction mixture. The mixture was stirred for 5 h at the

room temperature. Upon completion, the reaction was quenched with water and extracted with ethyl acetate. The combined organic phases were washed with water and brine, then dried and concentrated. The crude product was purified by silica gel column chromatography (petroleum ether/ethyl acetate, 6/1) to yield racemic compounds **11** as a white solid (1.40g, 48%).

4.2.8. *3-(6-Phenoxy pyridin-3-yl)-1-(piperidin-3-yl)-1H-pyrazolo[3,4-d]pyrimidin-4-amine hydrochloride (12)*

To a solution of racemic compounds **11** (0.49 g, 1 mmol) in THF (1 mL) was added 4M HCl in dioxane (5 mL) and the reaction mixture was stirred for 5 h at room temperature. The precipitate was filtrated, washed with ethyl acetate (25 mL) afforded racemic compounds **12** as a white solid (0.39 g, 92%).

4.2.9. *General procedure for the synthesis of 13a-13e*

To a solution of racemic compounds **12** (0.21 g, 0.5 mmol) and triethylamine (0.30 g, 1.5 mmol) in THF (20 mL), different acyl chloride (0.6 mmol) was added under ice-cold conditions and the mixture was stirred at room temperature for 5 h. Or to a solution of racemic compounds **12** (0.21 g, 0.5 mmol), HBTU (0.23g, 0.6 mmol) and triethylamine (0.30 g, 1.5 mmol) in THF (20 mL), different substituted acids (0.6 mmol) was added under ice-cold conditions and the mixture was stirred at room temperature for 8 h. Upon completion, the reaction was quenched with water and extracted with ethyl acetate. The combined organic phases were washed with water and brine, then dried and concentrated. The crude product was purified by silica gel column chromatography (dichloromethane/methanol, 100/1-60/1) to afford compounds **13a-13e**.

4.2.9.1. *1-(3-(4-Amino-3-(6-phenoxy pyridin-3-yl)-1H-pyrazolo[3,4-d]pyrimidin-1-yl)piperidin-1-yl)-2-hydroxyethan-1-one (13a)* White solid, yield 56%, Mp: 232-234 °C, ¹H NMR (400 MHz, DMSO-*d*₆) δ 8.30 (s, 1H), 8.20 (d, *J* = 6.8 Hz, 1H), 8.00 (d, *J* = 7.2 Hz, 1H), 7.38 (t, *J* = 7.8 Hz, 2H), 7.31 - 6.74 (m, 6H), 4.72 (t, *J* = 9.6 Hz, 0.5H), 4.65 - 4.57 (m, 0.5H), 4.54 (s, 0.5H), 4.41 (d, *J* = 11.7 Hz, 0.5H), 4.16 - 3.80 (m, 3H), 3.65 (d, *J* = 12.3 Hz, 0.5H), 3.55 - 3.45 (m, 0.5H), 3.12 (t, *J* = 11.5 Hz, 0.5H), 3.01 (t, *J* = 13.0 Hz, 0.5H), 2.93 - 2.81 (m, 0.5H), 2.23 - 2.11 (m, 1H), 2.06 (s, 1H), 1.82 (d, *J* = 12.6 Hz, 1H), 1.64 - 1.44 (m, 1H). ¹³C NMR (100 MHz, DMSO-*d*₆) δ 170.78, 170.60, 163.45, 158.71, 156.23, 154.57, 154.49, 154.37, 147.29, 141.15, 141.07, 140.46, 130.21,

125.08, 124.82, 121.56, 112.23, 98.14, 60.71, 60.62, 52.98, 52.63, 48.27, 46.04, 44.08, 41.95, 29.97, 29.89, 24.82, 23.77. MS(ESI) m/z: 446.16 [M + H]⁺

4.2.9.2. *1-(3-(4-Amino-3-(6-phenoxy)pyridin-3-yl)-1H-pyrazolo[3,4-d]pyrimidin-1-yl)piperidin-1-yl)-2-hydroxypropan-1-one (13b)* White solid, yield 62%, Mp: 165-168 °C, ¹H NMR (400 MHz, DMSO-*d*₆) δ 8.38 (s, 1H), 8.27 (s, 1H), 8.08 (d, *J* = 8.3 Hz, 1H), 7.46 (t, *J* = 7.7 Hz, 2H), 7.31 - 6.93 (m, 6H), 5.06 - 4.88 (m, 1H), 4.82 - 4.63 (m, 1H), 4.55 - 4.44 (m, 1H), 4.42 - 4.15 (m, 1.5H), 4.06 - 4.01 (m, 0.5H), 3.67 - 3.49 (m, 0.5H), 3.20 - 3.07 (m, 1H), 2.91 - 2.72 (m, 0.5H), 2.27 - 2.13 (m, 1H), 2.13 (s, 1H), 1.90 (s, 1H), 1.71 - 1.49 (m, 1H), 1.27 - 1.11 (m, 3H). ¹³C NMR (100 MHz, DMSO-*d*₆) δ 172.92, 172.80, 172.49, 163.45, 158.73, 156.24, 154.56, 154.47, 154.37, 147.29, 141.13, 140.45, 130.21, 125.07, 124.83, 121.55, 112.22, 98.16, 65.04, 64.91, 64.73, 53.42, 53.15, 52.78, 52.66, 49.21, 49.20, 46.24, 45.09, 45.07, 44.95, 42.09, 42.06, 42.04, 30.20, 30.06, 29.94, 25.15, 25.02, 24.13, 24.09, 21.34, 21.25, 21.08, 20.89. MS(ESI) m/z: 460.28 [M + H]⁺

4.2.9.3. *1-(3-(4-Amino-3-(6-phenoxy)pyridin-3-yl)-1H-pyrazolo[3,4-d]pyrimidin-1-yl)piperidin-1-yl)-3-hydroxy-2,2-dimethylpropan-1-one (13c)* White solid, yield 62%, Mp: 212-214 °C, ¹H NMR (400 MHz, DMSO-*d*₆) δ 8.31 (s, 1H), 8.19 (s, 1H), 8.01 (d, *J* = 8.4 Hz, 1H), 7.38 (t, *J* = 7.5 Hz, 2H), 7.32 - 6.77 (m, 6H), 4.64 (t, *J* = 10.6 Hz, 1H), 4.51 (t, *J* = 5.6 Hz, 1H), 4.39 (d, *J* = 12.2 Hz, 1H), 4.22 (d, *J* = 12.9 Hz, 1H), 3.36 (d, *J* = 5.6 Hz, 2H), 3.18 (t, *J* = 11.6 Hz, 1H), 2.89 (t, *J* = 12.0 Hz, 1H), 2.20 (q, *J* = 11.9 Hz, 1H), 2.04 (d, *J* = 9.9 Hz, 1H), 1.83 (d, *J* = 13.0 Hz, 1H), 1.53 (q, *J* = 12.5 Hz, 1H), 1.10 (d, *J* = 7.0 Hz, 6H). ¹³C NMR (100 MHz, DMSO-*d*₆) δ 174.92, 163.44, 158.73, 156.23, 154.48, 154.35, 147.29, 141.08, 140.46, 130.22, 125.14, 124.84, 121.56, 112.22, 98.16, 69.43, 53.03, 48.80, 45.21, 44.16, 30.07, 24.81, 23.43, 23.16. MS(ESI) m/z: 487.91 [M + H]⁺

4.2.9.4. *2-Methoxyethyl 3-(4-amino-3-(6-phenoxy)pyridin-3-yl)-1H-pyrazolo[3,4-d]pyrimidin-1-yl)piperidine-1-carboxylate (13d)* White solid, yield 58%, Mp: 152-154 °C, ¹H NMR (400 MHz, DMSO-*d*₆) δ 8.38 (s, 1H), 8.27 (d, *J* = 9.7 Hz, 1H), 8.08 (d, *J* = 8.4 Hz, 1H), 7.46 (t, *J* = 7.8 Hz, 2H), 7.40 - 6.83 (m, 6H), 4.82 - 4.72 (m, 0.5H), 4.68 - 4.59 (m, 0.5H), 4.52 (d, *J* = 12.1 Hz, 0.5H), 4.21 (d, *J* = 12.8 Hz, 0.5H), 4.06 (d, *J* = 12.4 Hz, 0.5H), 3.92 (d, *J* = 13.2 Hz, 0.5H), 3.65 - 3.45 (m, 2.5H), 3.22 (d, *J* = 13.2 Hz, 3H), 3.16 - 3.08 (m, 1H), 2.87 (t, *J* = 11.0 Hz, 0.5H), 2.71 - 2.56 (m, 1.5H), 2.46 - 2.41 (m, 0.5H), 2.28 - 2.20 (m, 1H), 2.12 (s, 1H), 1.89 (t, *J* = 13.8 Hz, 1H), 1.71 - 1.45 (m, 1H). ¹³C NMR (100 MHz, DMSO-*d*₆) δ 169.43, 169.30, 163.42, 158.72, 156.24, 156.22, 154.57,

154.44, 154.34, 147.28, 141.08, 140.98, 140.44, 130.20, 125.08, 124.83, 121.55, 112.20, 98.17, 98.10, 68.74, 58.45, 58.40, 53.20, 52.64, 45.73, 45.53, 33.13, 33.07, 30.05, 29.86, 25.09, 23.89. MS(ESI) m/z: 474.06 [M + H]⁺

4.2.9.5. *1-(3-(4-Amino-3-(6-phenoxy-pyridin-3-yl)-1H-pyrazolo[3,4-d]pyrimidin-1-yl)piperidin-1-yl)-2-chloroethan-1-one (13e)* White solid, yield 68%, Mp: 182-184 °C, ¹H NMR (400 MHz, DMSO-*d*₆) δ 8.37 (s, 1H), 8.27 (d, *J* = 7.0 Hz, 1H), 8.08 (d, *J* = 5.6 Hz, 1H), 7.46 (t, *J* = 7.8 Hz, 2H), 7.36 - 6.76 (m, 6H), 4.90 - 4.83 (m, 0.5H), 4.71 - 4.63 (m, 0.5H), 4.49 - 4.41 (m, 2H), 4.26 (d, *J* = 12.9 Hz, 0.5H), 4.17 (d, *J* = 11.1 Hz, 0.5H), 4.04 (d, *J* = 13.6 Hz, 0.5H), 3.85 (d, *J* = 13.0 Hz, 0.5H), 3.78 - 3.69 (m, 0.5H), 3.24 - 3.18 (m, 1H), 3.00 - 2.91 (m, 0.5H), 2.30 - 2.07 (m, 2H), 1.96 - 1.82 (m, 1H), 1.78 - 1.69 (m, 0.5H), 1.61 - 1.51 (m, 0.5H). ¹³C NMR (100 MHz, DMSO-*d*₆) δ 165.32, 165.28, 163.46, 158.72, 156.24, 154.62, 154.50, 154.37, 147.30, 147.26, 141.17, 141.11, 140.46, 140.40, 130.21, 125.07, 124.82, 121.55, 112.22, 98.20, 98.14, 52.97, 52.53, 49.72, 46.26, 45.91, 42.60, 42.47, 42.22, 30.02, 29.81, 24.84, 23.64. MS(ESI) m/z: 464.14 [M + H]⁺

4.3. *In vitro* BTK kinase activity assay and kinase selectivity assay

The *in vitro* BTK kinase activity and kinases selectivity activities were evaluated via a radiometric protein kinase assay²¹. All compounds were prepared to 50 X final assay concentration in 100% DMSO. A portion of this working stock of the compounds were added to the assay well as the first component in the reaction, followed by adding kinases dilution with specific buffer. The reaction was initiated by the addition of the Mg/ATP mix. After incubation for 40 minutes at room temperature, the reaction was stopped by the addition of phosphoric acid to a concentration of 0.5%. 10 μL of the reaction was then spotted onto a P30 filtermat and washed four times for 4 minutes in 0.425% phosphoric acid and once in methanol prior to drying and scintillation counting. IC₅₀ values were calculated using the Graphpad prism 6 software.

$$\text{activity rate \%} = \frac{\text{Count}_C - \text{Count}_B}{\text{Count}_P - \text{Count}_B} * 100\%$$

Count_C: the counts of testing compounds.

Count_P: the counts of positive control. The positive control wells contained all components of the reaction, except the compound of interest, and DMSO (at a final concentration of 2%) was

included in these wells to control for solvent effects.

Count_b: the counts of blank. The blank wells contained all components of the reaction with staurosporine replacing the compound of interest. This abolished kinase activity and established the baseline (0% kinase activity remaining).

4.4. Cell lines and primary MCL cells

MCL cell lines Mino, Jeko-1, Z138 and Maver-1 were purchased from the American Type Culture Collection (ATCC). Peripheral blood was obtained from MCL patients who provided informed consent. Mononuclear cells were separated by Ficoll-Hypaque density centrifugation, and tumor cells were isolated using anti-CD19 antibody coated magnetic microbeads (Miltenyi Biotec). Cells were cultured in RPMI-1640, supplemented with 10% heat-inactivated fetal bovine serum, 2% HEPES buffer and 1% penicillin (10,000 units/mL; Sigma), streptomycin (10 mg/mL; Sigma).

4.5. Cell proliferation assay

Cell proliferation assay was performed on MCL cell lines and primary MCL patient cells with the CellTiter-Glo Luminescent cell viability assay kit (Promega) following the manufacturer's protocol. In short, 50 μ L cells were plated in 96-well plates at a density of 1×10^4 cells/well for MCL cell lines and 12.5×10^4 cells/well for primary MCL patient cells, then treated with DMSO (control) and different concentrations of the synthesized compounds in triplicate and incubated in a humidified atmosphere with 5% CO₂ at 37 °C for 72 h on MCL cell lines and 24 h on primary MCL patient cells. Cells were lysed with 30 μ L Cell Titer-Glo Luminescent Cell Viability Assay Reagent (Promega, Madison, WI, USA), and luminescence was quantified using the BioTek Synergy HTX Multi-mode Micro Plate Reader (Winooski, VT, USA). Each triplicate experiment was performed no less than three times to establish the cell survival curve. IC₅₀ values were calculated using the Graphpad prism 6 software.

4.6. Western blotting

Z138 cells were cultured with 0.5 μ M and 1 μ M of **13e** and 1 μ M of **IBN** for 16 h. Then cells were harvested and lysed in a lysis buffer (Cell Signaling, Danvers, MA). The cell lysates were kept on ice for 30 min and centrifuged at $12,000 \times$ rpm for 20 min at 4 °C. The protein concentration was determined by the Bradford assay (Bio-Rad, Hercules, CA). Twenty micrograms of sample

proteins were mixed with the 4 × loading buffer and separated by 10% SDS-PAGE. The proteins were then transferred onto methanol equilibrated PVDF membrane (BIO-RAD Laboratories, 162e0177), which was blocked for 1 h in 5% nonfat dry milk in TBST (BD Bioscience, San Jose, CA). The membranes were incubated with a primary antibody overnight at 4 °C. Secondary antibodies were added for 1 h at room temperature. Finally, the membrane was visualized by ECL (Perkin Elmer Life Sciences, NE104001EA). Antibodies against BTK, PLC γ 2, p-BTK, p-PLC γ 2 and GAPDH were obtained from Cell Signaling.

4.7. Cell apoptosis assay

Apoptosis was quantified by Annexin V/Propidium Iodide (PI)- binding assay. Cells were seeded in 6-well plates with 1 μ M and 2 μ M of **13e** for 24 h. Treated cells were washed twice with cold phosphate-buffered saline (PBS) and then resuspended in 100 μ L binding buffer, to which 2 μ L of Annexin V-FITC and 5 μ L of PI were added. The samples were gently vortexed and incubated for 15 min at room temperature in the dark. After addition of 200 μ L binding buffer, samples were immediately analyzed by flow cytometry using a FACScan flow cytometer (Becton Dickinson, San Jose, CA). The number of apoptotic cells was determined using the Flowjo software.

4.8. Stability in human liver microsomes

In vitro metabolic stability in human liver microsomes was assessed using testosterone, diclofenac, and propafenone as control. A DMSO solution of the tested compound (10 mm, 10 μ L/well) and solution of microsome (80 μ L/well) were added to a 96-well plate; this mixture was first incubated at 37 °C for 10 min. Then potassium phosphate buffer (100 mm, 10 μ L/well) was added, and no cofactor (NCF) remaining was evaluated after a further incubation of 60 min. After this prewarming process, NADPH regenerating system (10 μ L/well) was added, and remaining of each compound was tested at five time-points (5, 10, 20, 30 and 60 min). At each timepoint, stop solution (including 100 ng/ml tolbutamide and 100 ng/ml labetalol, cold in 4 °C, 300 μ L/well) was added to terminate the reaction. The sampling plates were shaken for approximate 10 min, and then samples were centrifuged at 1306 g for 20 min under 4 °C to afford the supernatant (100 μ L) for LC/MS test. Intrinsic clearance (CL_{int}) and half-life ($T_{1/2}$) values were then calculated. $CL_{int}(\text{mic}) = 0.693 / \text{half-life/mg microsome protein per ml}$. $CL_{int}(\text{liver}) = CL_{int}(\text{mic}) \times (45 \text{ mg microsomal protein/g liver weight}) \times (20 \text{ g liver weight/kg body weight})$.

4.9. Molecular docking

Molecular docking was performed using the Sybyl 2.0 software and the BTK crystal structure (PDB: 5P9I) was retrieved from the Protein Data Bank. Protein preparation was performed by extracting the ligand, removing water molecules, adding hydrogen atoms and assigning AMBER7 FF99 charges to the protein. Compound **13e** was docked into BTK and the hydrogen bonds and hydrophobic interactions were observed in the model, the best conformation with the highest CScore was selected for interaction analysis.

4.10. Statistical analysis

Student's tests were performed for statistical analyses of **13e** induced apoptotic effect, two-way ANOVA analysis of variance was used to compare the **IBN** and **13e** treatment in the primary patient cells *in vitro*. P values of <0.05 were considered statistically significant.

Acknowledgements

This work was supported by the key research and development project of Shandong Province [No. 2017CXGC1401].

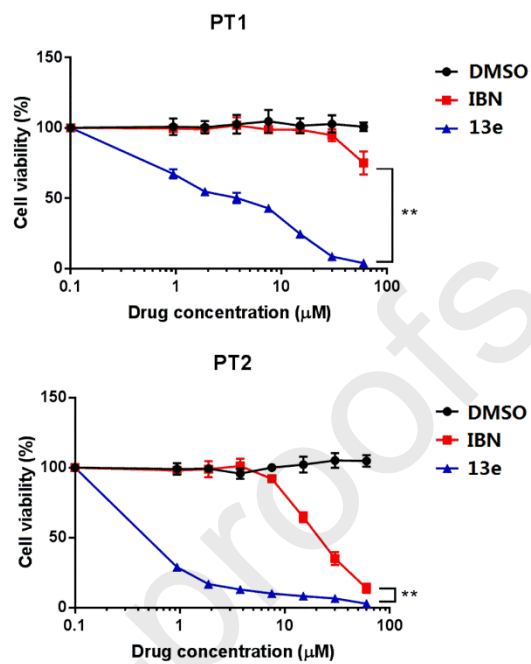
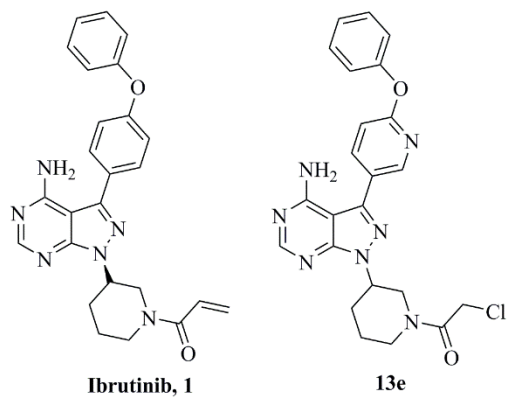
References:

1. C.M. Lewis, C. Broussard, M.J. Czar, P.L. Schwartzberg, Tec kinases: modulators of lymphocyte signaling and development, *Curr. Opin. Immunol.* 13 (2001) 317-325, [https://doi.org/10.1016/S0952-7915\(00\)00221-1](https://doi.org/10.1016/S0952-7915(00)00221-1)
2. R. Kuppers, Mechanisms of B-cell lymphoma pathogenesis, *Nat. Rev. Cancer* 5 (2005) 251-262, <https://doi.org/10.1038/nrc1589>
3. Z. Zhang, D.G. Zhang, Y. Liu, D.Z. Yang, F.S. Ran, M.L. Wang, G.S. Zhao, 2018. Targeting Bruton's tyrosine kinase for the treatment of B cell associated malignancies and autoimmune diseases: Preclinical and clinical developments of small molecule inhibitors. *Arch. Pharm.* 351, e1700369, <https://doi.org/10.1002/ardp.201700369>
4. J.J. Buggy, L. Elias, Bruton Tyrosine Kinase (BTK) and Its Role in B-cell Malignancy, *Int. Rev. Immunol.* 31 (2012) 119-132, <https://doi.org/10.3109/08830185.2012.664797>
5. R.H. Advani, J.J. Buggy, J.P. Sharman, S.M. Smith, T.E. Boyd, B. Grant, K.S. Kolibaba, R.R. Furman, S. Rodriguez, B.Y. Chang, J. Sukbuntherng, R. Izumi, A. Hamdy, E. Hedrick, N.H. Fowler, Bruton Tyrosine Kinase Inhibitor Ibrutinib (PCI-32765) Has Significant Activity in Patients With Relapsed/Refractory B-Cell Malignancies, *J. Clin. Oncol.* 31 (2013) 88-94, <https://doi.org/10.1200/JCO.2012.42.7906>
6. R.E. Davis, V.N. Ngo, G. Lenz, P. Tolar, R.M. Young, P.B. Romesser, H. Kohlhammer, L. Lamy, H. Zhao, Y.D. Yang, W.H. Xu, A.L. Shaffer, G. Wright, W.M. Xiao, J. Powell, J.K. Jiang, C.J. Thomas, A. Rosenwald, G. Ott, H.K. Muller-Hermelink, R.D. Gascoyne, J.M. Connors, N.A. Johnson, L.M. Rimsza, E. Campo, E.S. Jaffe, W.H. Wilson, J. Delabie, E.B. Smeland, R.I. Fisher, R.M. Braziel, R.R.

- Tubbs, J.R. Cook, D.D. Weisenburger, W.C. Chan, S.K. Pierce, L.M. Staudt, Chronic active B-cell-receptor signalling in diffuse large B-cell lymphoma, *Nature* 463 (2010) 88-92, <https://doi.org/10.1038/nature08638>
7. J.H. Lv, J.D. Wu, F. He, Y. Qu, Q.Q. Zhang, C.G. Yu, Development of Bruton's tyrosine kinase Inhibitors for Rheumatoid Arthritis, *Curr. Med. Chem.* 25 (2018) 5847-5859, <https://doi.org/10.2174/0929867325666180316121951>
 8. R.C. Rickert, New insights into pre-BCR and BCR signalling with relevance to B cell malignancies, *Nat. Rev. Immunol.* 13 (2013) 578-591, <https://doi.org/10.1038/nri3487>
 9. F.S. Ran, Y. Liu, D.G. Zhang, M.X. Liu, G.S. Zhao, Discovery of novel pyrazole derivatives as potential anticancer agents in MCL, *Bioorg. Med. Chem. Lett.* 29 (2019) 1060-1064, <https://doi.org/10.1016/j.bmcl.2019.03.005>
 10. R.M. Young, L.M. Staudt, Targeting pathological B cell receptor signalling in lymphoid malignancies, *Nat. Rev. Drug. Discov.* 12 (2013) 229-243, <https://doi.org/10.1038/nrd3937>
 11. M. Cinar, F. Hamedani, Z.C. Mo, B. Cinar, H.M. Amin, S. Alkan, Bruton tyrosine kinase is commonly overexpressed in mantle cell lymphoma and its attenuation by Ibrutinib induces apoptosis, *Leukemia Res.* 37 (2013) 1271-1277, <https://doi.org/10.1016/j.leukres.2013.07.028>
 12. B.Y. Chang, M. Francesco, M.F.M. De Rooij, P. Magadala, S.M. Steggerda, M.M. Huang, A. Kuil, S.E.M. Herman, S. Chang, S.T. Pals, W. Wilson, A. Wiestner, M. Spaargaren, J.J. Buggy, L. Elias, Egress of CD19(+)CD5(+) cells into peripheral blood following treatment with the Bruton tyrosine kinase inhibitor ibrutinib in mantle cell lymphoma patients, *Blood* 122 (2013) 2412-2424, <https://doi.org/10.1182/blood-2013-02-482125>
 13. M.L. Wang, S. Rule, P. Martin, A. Goy, R. Auer, B.S. Kahl, W. Jurczak, R.H. Advani, J.E. Romaguera, M.E. Williams, J.C. Barrientos, E. Chmielowska, J. Radford, S. Stilgenbauer, M. Dreyling, W.W. Jdrzejczak, P. Johnson, S.E. Spurgeon, L. Li, L. Zhang, K. Newberry, Z.S. Ou, N. Cheng, B.L. Fang, J. McGreivy, F. Clow, J.J. Buggy, B.Y. Chang, D.M. Beaupre, L.A. Kunkel, K.A. Blum, Targeting BTK with Ibrutinib in Relapsed or Refractory Mantle-Cell Lymphoma, *New Engl. J. Med.* 369 (2013) 507-516, <https://doi.org/10.1056/NEJMoa1306220>
 14. A. Noy, S. De Vos, C. Thieblemont, P. Martin, C.R. Flowers, F. Morschhauser, G.P. Collins, S. Ma, M. Coleman, S. Peles, S. Smith, J.C. Barrientos, A. Smith, B. Munneke, I. Dimery, D.M. Beaupre, R. Chen, Targeting BTK with Ibrutinib in Relapsed/ Refractory Marginal Zone Lymphoma, *Blood* 129 (2017) 2224-2232, <https://doi.org/10.1182/blood-2016-10-747345>
 15. Z.Y. Pan, H. Scheerens, S.J. Li, B.E. Schultz, P.A. Sprengeler, L.C. Burrill, R.V. Mendonca, M.D. Sweeney, K.C.K. Scott, P.G. Grothaus, D.A. Jeffery, J.M. Spoerke, L.A. Honigberg, P.R. Young, S.A. Dalrymple, J.T. Palmer, Discovery of selective irreversible inhibitors for Bruton's tyrosine kinase, *Chemmedchem* 2 (2007) 58-61, <https://doi.org/10.1002/cmdc.200600221>
 16. X.G. Zhao, M.H. Xin, Y.Z. Wang, W. Huang, Q. Jin, F. Tang, G. Wu, Y. Zhao, H. Xiang, Discovery of thieno[3,2-c]pyridin-4-amines as novel Bruton's tyrosine kinase (BTK) inhibitors, *Bioorg. Med. Chem.* 23 (2015) 6059-6068, <https://doi.org/10.1016/j.bmc.2015.05.043>
 17. A.R. Johnson, P.B. Kohli, A. Katewa, E. Gogol, L.D. Belmont, R. Choy, E. Penuel, L. Burton, C. Eigenbrot, C. Yu, D.F. Ortwine, K. Bowman, Y. Franke, C. Tam, A. Estevez, K. Mortara, J.S. Wu, H. Li, M. Lin, P. Bergeron, J.J. Crawford, W.B. Young, Battling Btk Mutants With Noncovalent Inhibitors That Overcome Cys481 and Thr474 Mutations, *Acs. Chem. Biol.* 11 (2016) 2897-2907, <https://doi.org/10.1021/acscchembio.6b00480>
 18. C. Liang, D. Tian, X. Ren, S. Ding, M. Jia, M. Xin, S. Thareja, The development of Bruton's

- tyrosine kinase (BTK) inhibitors from 2012 to 2017: A mini-review, *Eur. J. Med. Chem.* 151 (2018) 315-326, <https://doi.org/10.1016/j.ejmech.2018.03.062>
19. L. He, H. Pei, C. Zhang, M. Shao, D. Li, M. Tang, T. Wang, X. Chen, M. Xiang, L. Chen, Design, synthesis and biological evaluation of 7H-pyrrolo[2,3-d]pyrimidin-4-amine derivatives as selective Btk inhibitors with improved pharmacokinetic properties for the treatment of rheumatoid arthritis, *Eur. J. Med. Chem.* 145 (2018) 96-112, <https://doi.org/10.1016/j.ejmech.2017.12.079>
20. J. Liu, D. Guiadeen, A. Krikorian, X. Gao, J. Wang, S.B. Boga, A.B. Alhassan, Y. Yu, H. Vaccaro, S. Liu, C. Yang, H. Wu, A. Cooper, J. De Man, A. Kaptein, K. Maloney, V. Hornak, Y.D. Gao, T.O. Fischmann, H. Raaijmakers, D. Vu-Pham, J. Presland, M. Mansueto, Z. Xu, E. Leccese, J. Zhang-Hoover, I. Knemeyer, C.G. Garlisi, N. Bays, P. Stivers, P.E. Brandish, A. Hicks, R. Kim, J.A. Kozlowski, Discovery of 8-Amino-imidazo[1,5-a]pyrazines as Reversible BTK Inhibitors for the Treatment of Rheumatoid Arthritis, *ACS. Med. Chem. Lett.* 7 (2016) 198-203, <https://doi.org/10.1021/acsmchemlett.5b00463>
21. F.S. Ran, Y. Liu, M.X. Liu, D.G. Zhang, P. Wang, J.Z. Dong, W.D. Tang, G.S. Zhao, Discovery of pyrazolopyrimidine derivatives as potent BTK inhibitors with effective anticancer activity in MCL, *Bioorganic Chemistry* (2019), <https://doi.org/10.1016/j.bioorg.2019.102943>

Graphical abstract



Highlights:

- **13e** explained potent BTK inhibitory activity.
- **13e** obtained antiproliferative effects in primary patient tumor cells.
- **13e** showed more potent antitumor effects in mantle cell lymphoma than ibrutinib.
- **13e** could completely inhibit the phosphorylation of BTK and PLC γ 2 in Z138 cells at low micromolar concentration.
- Low micromolar doses of **13e** induced strong cell apoptosis in Jeko-1 and Z138 cells.